Impact of demand-side management on the sizing of autonomous solar PV-based mini-grids

Energy 278 (2023) 127884

Contents lists available at ScienceDirect

Energy

journal homepage: www.elsevier.com/locate/energy

Impact of demand-side management on the sizing of autonomous solar PV-based mini-grids

Milky Ali Gelchu [a], Jimmy Ehnberg [b], Dereje Shiferaw [a], Erik O. Ahlgren [c,*]

[a] School of Electrical and Computer Engineering, Addis Ababa University, Addis Ababa, Ethiopia
[b] Department of Electrical Engineering, Chalmers University of Technology, Gothenburg, Sweden
[c] Department of Space, Earth, and Environment, Chalmers University of Technology, Gothenburg, Sweden

ARTICLE INFO

Handling Editor: Dr. Henrik Lund

Keywords:
Demand-side management
Load flexibility
Solar PV
Mini-grid
Particle swarm optimization

ABSTRACT

Solar PV-based autonomous mini-grids represent an economically affordable and robust electrification option for rural communities. However, the initial investment cost for renewable energy technologies such as solar PV remains high for rural communities. Implementation of demand-side management (DSM) could increase the cost-efficiency of mini-grids in rural areas. This requires demand-side knowledge, but little is still known of electricity demands in recently electrified areas and, in particular, of how DSM implementation could impact mini-grids. The few studies available focus either on systems or on appliance levels while this study aims to determine cost-efficiency impacts of DSM implementation at a category level. A shifting strategy is applied based on classification into high priority loads and low priority loads. Autonomous rural mini-grid components sizing for four different load categories and load flexibility are carried out using particle swarm optimization. The results show that different load category combinations result in large variations in terms of possible levelized energy cost reductions and, thus, in terms of the cost-optimal sizing of the mini-grid components. The DSM implementation on the household and productive use categories have the largest capacity of reducing the levelized energy cost, by 45.8% and 20.7%, respectively, compared to the no demand-side management case.

Credit author statement

We certify that all authors have participated sufficiently in this research work from intellectual conception, and design of the research objectives, analysis and interpretation of the result and writing of the manuscript. The contribution of each author is provided hereafter. Milky Ali Gelchu: Conceptualization, Methodology, Software, Writing-Original Draft and Writing - Review and Editing. Jimmy Ehnberg: Conceptualization, Supervision, Reviewing, and Editing. Dereje Shiferaw: Conceptualization, Supervision, Reviewing, and Editing. Erik O. Ahlgren: Conceptualization, Supervision, Writing – Review, and Editing.

1. Introduction

Access to affordable electricity is a vital enabling factor for human development, and improving this access in developing countries is one part of the seventh United Nations Sustainable Development Goal (UNSDG) [1]. One billion people, representing 13% of the world's population, lacked access to electricity in Year 2017. Roughly half of these people live in sub-Saharan Africa (SSA), with a large majority inhabiting rural areas [2]. UNSDG stipulates the need for an innovative sustainable energy transformation for rural areas [1].

Autonomous mini-grids constitute an economically affordable and robust electrification option for non-electrified areas in which extensions to the electric grid are not techno-economically feasible [3]. Mini-grids are electric power generation and distribution systems that provide electricity to a few customers in a remote settlement or bring power to hundreds of thousands of customers in a town or city. Mini-grids can be either fully isolated from the national grid (autonomous) or connected to it [4].

Mini-grids are a fundamental "building block of the Smart Grid" [5]. Studies define the term "Smart Grid" in various ways, but most of the definitions share the idea that the Smart Grid is a stable, efficient and reliable system [6]. Among the definitions, the European Technology Platform defines a Smart Grid as: "*an electricity network that can intelligently integrate the actions of all users connected to it - generators,*

* Corresponding author.
E-mail addresses: themilk8@gmail.com (M.A. Gelchu), jimmy.ehnberg@chalmers.se (J. Ehnberg), dnderejesh@gmail.com (D. Shiferaw), erik.ahlgren@chalmers.se (E.O. Ahlgren).

https://doi.org/10.1016/j.energy.2023.127884
Received 5 January 2023; Received in revised form 14 April 2023; Accepted 18 May 2023
Available online 19 May 2023

consumers, and those that do both to efficiently deliver sustainable, economic, and secure electricity supplies" [7].

In recent years, the capital costs of renewable energy technologies (RETs) have been decreasing [3]. Among RETs, solar photovoltaic (PV) systems are gaining traction in SSA [4], although costs in SSA are still much higher than the world average due to political, financial, and technological risks [8].

There are many non-electrified areas in SSA countries receiving high levels of solar irradiation. E.g. Ethiopia, with an rural electricity access rate of 27%, has a potential total solar electricity reserve of 2.199 million TWh/annum with average insolation level of 5.25 kWh/m^2 [9]. Thus, solar PV- and battery energy storage (BES)-based autonomous mini-grids represent potential sustainable and reliable solutions for the electrification of rural areas [10].

The initial investment cost for solar PVs remains high for rural communities, and financial viability has been achieved until now only through heavy subsidization of this cost [11]. Consequently, in SSA, private stakeholders have been reluctant to invest in mini-grids due to the high level of uncertainty and the uncertain investment risk-return profile [12].

Mini-grid supply-side optimization and component sizing have been studied with different optimization methods in order to overcome the aforementioned barriers to mini-grid investments. While an iterative optimization technique for solar PV system sizing has been presented [13], it is usually time-consuming and may not provide accurate results. The Hybrid Optimization of Multiple Energy Resources (HOMER) software has been used for sizing hybrid renewable energy sources (HRES) [14]. However, it lacks flexibility in relation to altering the operating strategy and objective function.

In supply-side optimization studies, heuristic optimization algorithms have also been used, including a dynamic programming algorithm used for sizing of energy storage [5], a genetic algorithm (GA) used for optimal sizing of a PV-diesel-battery system [15], Non-dominated Sorting Genetic Algorithm (NSGA-II) used for HRES sizing based on different objectives [16], Virus Colony Search (VCS) algorithm [17], metaheuristic Gray Wolf Optimization (GWO) algorithm [18], and Particle Swarm Optimization (PSO) algorithms used for optimal sizing of different renewable energy source combinations [19–21]. The PSO algorithm yields high-quality solutions in a shorter simulation time than the iterative, HOMER, and most of the heuristic algorithms described above [20,22].

In recent years, machine learning algorithms are also used in supply-side optimization. They have short computational time and high exploration efficiency compared to heuristic algorithms. However, machine learning algorithms require significant amounts of historical data at the training stage [23].

On the supply side, the output of renewable energy sources (RES) is variable and is not known with perfect accuracy (referred to as 'uncertainty') [24]. This uncertainty necessitates the incorporation of expensive BES to minimize the effects of intermittence [25], the installation of additional generation capacity, or load flexibility [17]. There are also demand variations on sub-hourly, hourly, daily, and/or seasonal timeframes [26].

Flexibility is the ability of the system to cope with variations in generation and load. Flexibility cannot be provided solely by flexible generation units, e.g., hydropower or gas power, as it also requires a set of policies and control methods to manage the electrical loads, referred to as Demand-Side Management (DSM) [7]. Load flexibility can involve the shifting of the electricity demand to another time to offset the peak demand or to maximize the use of electricity from RES [26].

DSM is a Smart Grid strategy that enables the interaction between consumer and utility, being geared towards improving energy efficiency through demand profile modifications. There are six broadly discussed and implemented techniques for DSM including: peak clipping, valley filling, load shifting, load building, strategic conservation, and strategic load growth [27]. Load shifting, which is the most commonly used DSM strategy, is performed by load categorization based on various criteria [27].

Different studies examined how DSM implementation for different load profiles affects the cost-effectiveness of mini-grids. Optimized demand combinations that can be met using the available supplied power to reduce the cost of electricity [28,29]. DSM-based optimization was proposed and implemented for HRES sizing to reduce the initial capital cost of mini-grids [11]. Smart Grid concept-based load management, which divides the load profile into high and low priority loads, was applied for HRES sizing for electricity cost minimization [30]. An energy management strategy was proposed and implemented with DSM to minimize the operating cost of energy storage system of mini-grid [31]. DSM was implemented by using a flexible load priority list to minimize the operational cost without shedding critical loads in a mini-grid [32]. DSM using load shifting and frequency-based pricing was proposed to maximize utilization of renewable resources and system frequency [33].

The demand response (DR) program is a branch of DSM that aims to motivate and influence electricity consumers to reshape their energy demands in return for benefits offered by utility companies [25]. The impact of DR has been studied with different objectives, for instance, for total cost reduction [17], for financial and load balancing [34], to achieve supply–demand balance and increase profit of power suppliers [35], and for power system planning using techno-economical optimization to reduce the total cost [36].

The above-presented studies investigated the impact of DSM on the cost-efficiency of HRES-based mini-grids rather than that of 100% RES-based autonomous mini-grids. Further, the impacts of DSM implementation strategies have been studied either at the system level or appliance level, e.g., household appliances [11,28–30], but the control of each appliance is not an easy task as every appliance needs to be connected to the controller through cable or communication networks, especially in rural areas [27]. Thus, for the full exploitation of DSM implementation in rural areas, a low cost control and communication network infrastructure is essential [37].

In the aforementioned studies, even if the impact of DSM on the cost-efficiency of mini-grids was determined by incorporating DSM into the mini-grid sizing methodology, there were no consideration of the load-side uncertainties related to inaccurate load profile estimations or of the supply-side uncertainties linked to intermittency. Some studies have examined the effects of such uncertainties in relation to DSM implementation for mini-grids sizing and shown that the load and supply-side uncertainties impacts the optimum economic and reliability design of mini-grids, but the uncertainties were modeled differently in the studies [16,17,38,39]. For example, one study [16] used Chance Constrained Programming (CCP) to address the supply-side uncertainties, whereas another study [38] used CCP to model both the load-side and supply-side uncertainties. Uncertainties linked to both the load and supply sides have also been modeled using different distribution functions [17,39].

Based on the identified knowledge gaps, this study investigates the potential impact on cost-efficiency of DSM implementation by addressing different load categories (rather than looking only at the appliance level). In addition, the impacts on cost-efficiency of DSM implementation and load flexibility are compared.

The main research questions addressed in this study are:

- What is the impact of DSM implementation at the category level on the cost-efficiencies of solar PV and HRES-based autonomous mini-grids in rural areas?
- How large is the impact of DSM implementation at the category level on the cost-efficiencies of solar PV and HRES-based autonomous mini-grids in rural areas, as compared to the impact of load flexibility?

The remainder of this paper is structured as follows. The method used, configurations, and modeling of the components of the mini-grid

are described in Section 2. Section 3 describes the data used, section 4 describes the results and analysis, section 5 discusses the results and section 6 draws some overall conclusions from the work.

2. Method

The electricity demand distribution in rural areas of SSA is characterized by dispersed consumers, low consumption, and low income levels of the consumers [40]. Low income levels affect the willingness to pay for electricity, which in turn depends on the electricity tariff, in that strong willingness to pay is associated with a low electricity tariff [41]. Thus, the impact of DSM implementation at the category level on the sizing of a cost-efficient, solar PV-based, autonomous mini-grid is determined on the basis of levelized energy cost (LEC) minimization.

The optimal, cost-efficient sizing of autonomous mini-grid components based on LEC minimization is determined using a PSO algorithm, characterized by easy implementation, robustness, computation efficiency compared with other existing heuristic algorithms and exhibiting good performance in solving these types of problems [22,42]. To validate the results obtained from the PSO algorithm an iterative method is used.

To study the impact of DSM implementation at the category level on the configuration of the autonomous mini-grid, two different configurations are used. Similarly, the impact of DSM implementation at the category level is compared with load flexibility by determining the optimal sizing of autonomous mini-grid components. For this, conditions representing a village in northeastern Ethiopia is used.

In the following sections, the demand categorization, mini-grid configurations used, problem formulation, operating strategy used for DSM, method of optimization, and the modeling of mini-grid components are described.

2.1. Demand categorization

In a static model of the load profiles in the rural mini-grids, the productive use and community types of electricity consumers have been shown to present different load profile patterns than the household consumers [27]. These different load profile patterns can be used to design a financial incentive entailing different tariff settings for different load categories to encourage load-shifting from peak to off-peak periods (time-of-use tariffs), which is the most effective measure to implement DSM.

To determine the impact of DSM on the cost efficiency of an autonomous rural mini-grid, this study proposes the implementation of DSM for four load categories with different load profile patterns. The four load categories are: household loads (C-1); community loads (C-2); productive use (PU) loads having night time load (C-3); and PU loads not having night time load (C-4).

The sizing of mini-grids requires knowledge of the electricity load profile [43]. Load profiles may exhibit variability. However, most of the variations are limited in developing SSA countries, since weather conditions are similar throughout the year and social behaviors are essentially unchanging [44]. In the sizing of a cost-efficient autonomous mini-grid system, weekly load profiles are used for each load category.

To model the weekly load profile for each load category, a bottom-up methodology is applied. The load profiles are estimated based on data collected by the Ethiopian Electric Utility (EEU), the state-owned power utility. The collected data include appliance type and number, power rating, and probability of being used. An appliance-specific load profile is estimated for each appliance by multiplying the appliance power rating by the appliance probability of use. A load profile for each load category is estimated by summing up the appliance-specific load profiles.

2.2. Configurations

Two configurations of an autonomous mini-grid are used. Configuration 1 contains only solar PV and BES and is, thus, a 100% RES-based autonomous mini-grid. Configuration 2 represents a HRES-based autonomous mini-grid in which a diesel generator (DG) is added to the solar PV and BES. A schematic of the autonomous mini-grid system with both configurations is presented in Fig. 1.

2.3. Problem formulation

In this study, the impact of DSM implementation at category level on the cost-efficiency of mini-grid is formulated as an optimization problem, which determines the component sizing using a priority-based load shifting strategy. The objective function is minimization of the LEC. To determine the impact difference among the load categories, sixteen combinations of the four load categories are compared with the No DSM case (i.e., mini-grid component sizing without load prioritization) in a priority-based fashion. For comparison of the impact of DSM implementation at a category level with load flexibility, different percentages of load flexibility for the two configurations are used. The load flexibility at each hour t determines the amount of electricity load that is shiftable. The shiftable load which is considered a low-priority load in the implemented DSM operating strategy is calculated using Eq. (1):

$$L(t) = P(t) \times Lf \tag{1}$$

where $L(t)$ is the flexible load at hour t, $P(t)$ is the load at hour t, and Lf is the percentage of load flexibility.

To increase the robustness of the optimization problem, load-side uncertainties related to inaccurate load profile estimations and supply-side uncertainties related to intermittency are considered. To determine how the uncertainties impact the mini-grid sizing, component sizing with and without uncertainties considered is calculated. In addition, the validation of the results is examined using an iterative method. In determining the impact of uncertainties and validation of the results using an iterative method, a 10% load flexibility case is used. The objective function and constraints used for this study are explained in the following sections.

2.3.1. Objective function

The levelized energy cost (LEC) is the objective function of the optimization problem. It is an indicator for the cost-reflective tariff and is calculated as:

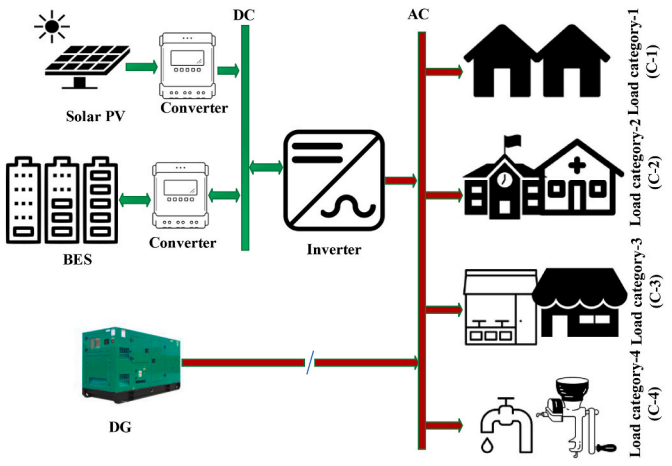

Fig. 1. Schematic of the autonomous mini-grid system, showing the load categories for Configurations 1 and 2.

$$LEC = \frac{TPV \times CRF}{LAE} \quad (2)$$

where *LAE* is the annual load demand (the summation of all demand per year), and *CRF* is the capital recovery factor, which depends on the rate of annual interest (r) and plant life (T). *TPV* is the total present cost of the entire system and is calculated as:

$$TPV = IC + OMC + RC + FC - PSV \quad (3)$$

where *IC* is the initial capital cost, *OMC* is the operation maintenance cost, *RC* is the replacement cost, *FC* is the fuel costs, and *PSV* is the present scrappage value of the mini-grid components. The initial capital cost includes the component price, the cost of civil work, and the installation cost for the autonomous mini-grid components.

The fuel cost of the DG is calculated as:

$$FC = D_f(t) DG_h P_f \quad (4)$$

where DG_h is the total operating hours of the DG during time *T*, and P_f is the fuel price per liter [30].

2.3.2. Design constraints

The mini-grid sizing is subject to various constraints. Security constraints to enforce the autonomous mini-grid should cover the required energy demand-supply and are expressed as:

$$E_{dem} \leq E_{sup} \quad (5)$$

where E_{dem} and E_{sup}, respectively, are the total energy demand required and the total energy demand supplied in the autonomous mini-grid.

In addition, there is the BES constraint: the state of charge of a BES (SOC) at any time *t* should lie between the minimum (SOC_{min}) and the full capacity of the BES (SOC_{max}). This limit of a state of charge is expressed by Eq. (6), where the maximum charge quantity of the BES (SOC_{max}) takes the value of the nominal capacity of the BES (C_B), and the minimum charge quantity of the BES (SOC_{min}), is determined using the maximum depth of discharge (DOD):

$$SOC_{min} \leq SOC(t) \leq SOC_{max} \quad (6)$$

2.4. Operating strategy

A load-shifting strategy operating strategy is used to manage load categories in a priority-based fashion based on a classification into high-priority loads (HPLs) and low-priority loads (LPLs). HPLs are non-shiftable loads and are, therefore, allowed to operate at their scheduled time by the user. In contrast, LPLs are shiftable loads which can be shifted to a time when there is sufficient electric power generation from solar PV and the BES is full. The maximum allowed shifting time is 24 h. Thus, the used operating strategy maximizes the hours of energy served for HPLs and minimizes them for LPLs. The flowcharts of the operating strategies used for Configurations 1 and 2 are shown in Figs. 2 and 3, respectively.

The step-by-step description of the flowchart used for the configurations operational strategy is as follows. For Configuration 1, the electrical power from solar PV in hour *t*, ($P_{pv}(t)$), is first used to satisfy the HPL in that hour, and the remaining energy, ($P_{BC}(t)$), expressed based on the efficiency of the inverter (η_{inv}), if any, is added to the available energy in the BES (charging) from the previous period. This stored energy is used to supply the HPLs during the period when the electrical power generated from solar PV is insufficient to satisfy (discharging) $P_{BD}(t)$. However, the state of charge of the BES (SOC), expressed based on the BES self-discharge rate (σ), is less than the maximum state of charge (SOC_{max}) during charging, and the BES must be above its minimum state of charge (SOC_{min}) during discharge. The

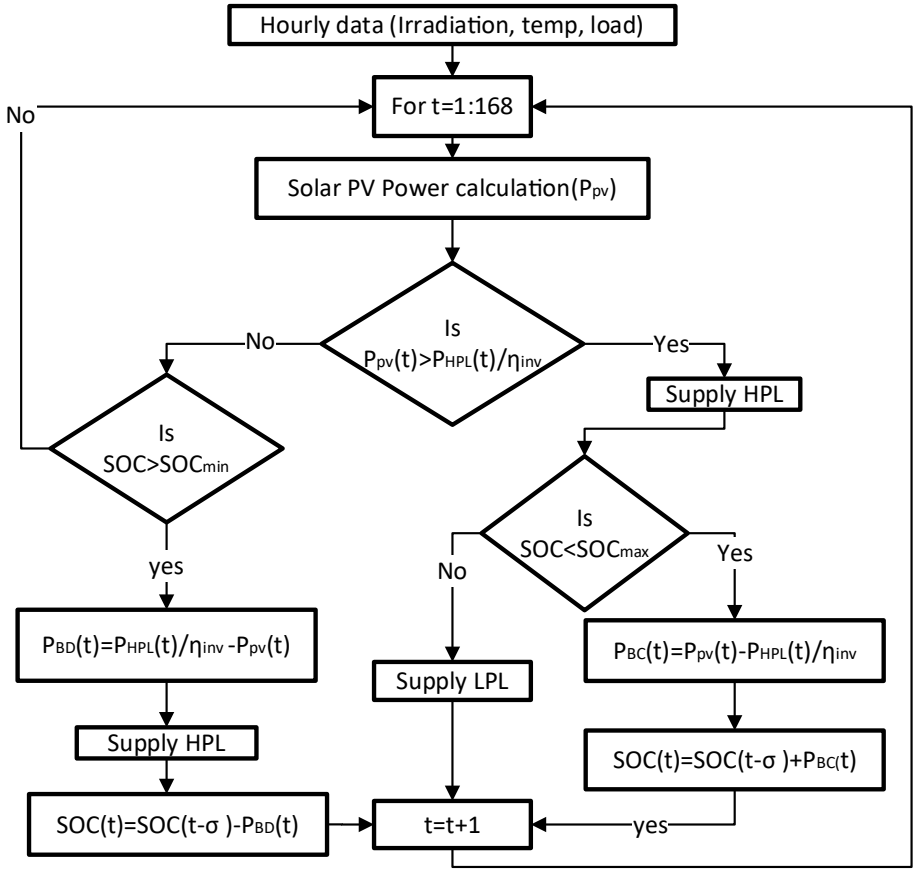

Fig. 2. Flowchart of the operating strategy for Configuration 1.

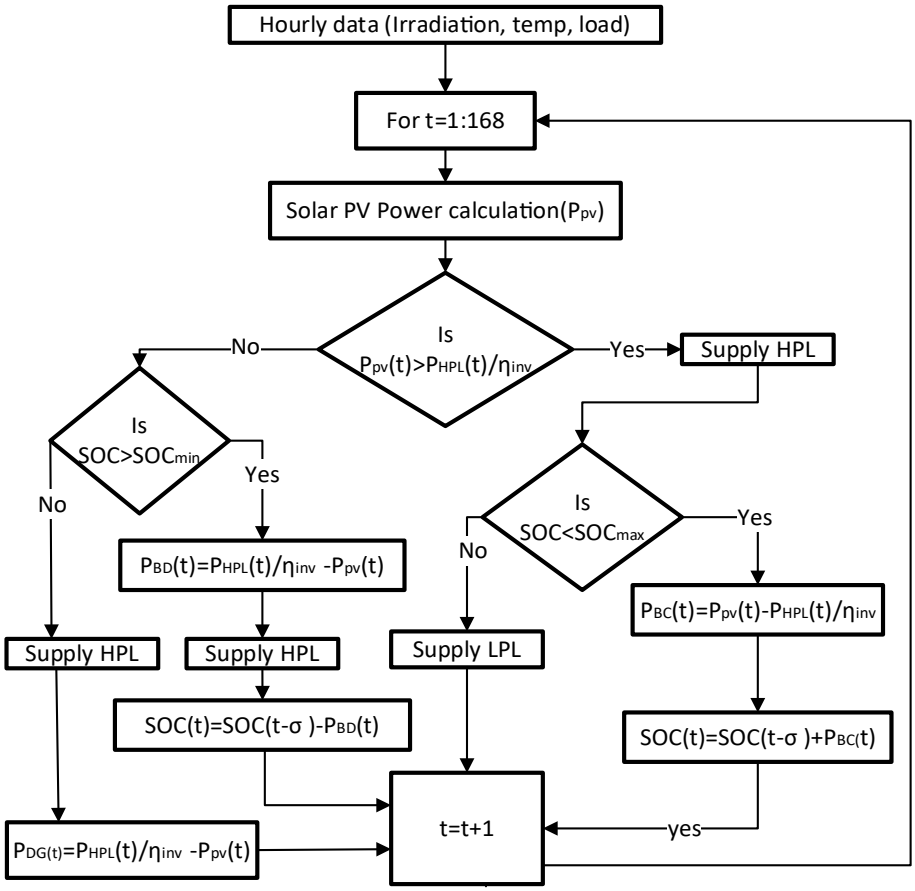

Fig. 3. Flowchart of the operating strategy for Configuration 2.

LPLs are supplied when there is excess energy from solar PV and the BES is equal to SOC_{max}. Thus, the LPL is shifted to a time where there is sufficient electricity generation from the solar PV and the BES is equal to SOC_{max}.

All the steps described for Configuration 1 are applied in Configuration 2, with the exception that the electrical power generated from solar PV and stored energy in the BES is not sufficient to supply the HPL, which means that in this case the HPLs will be supplied using the DG ($P_{DG}(t)$).

2.5. Method of optimization

The PSO algorithm is used to identify the optimal sizes of the components of the autonomous mini-grid, while minimizing the LEC as an objective function using the MATLAB software.

PSO is one of the most popular heuristic optimization algorithms used to solve optimization problems. In the PSO algorithm (Fig. 4), each particle (swarm) represents a potential solution, and these solutions are assessed by the optimization objective function to determine their fitness. In the PSO algorithm, each particle modifies its movement according to the best position achieved previously by the particle (X_i^p) and the global best (X_i^p) position of the entire population (to which it belongs) [45,46].

The two equations used for PSO are the position update equation [Eq. (7)] and the velocity update equation, [Eq. (8)]. These are to be modified in each iteration of the PSO algorithm, so as to converge to the optimum.

$$V_i(t+1) = \mathrm{w}V_i(t) + C_1 r_1 (X_i^p(t) - X_i(t)) + C_2 r_2 (X_i^g(t) - X_i(t)) \quad (7)$$

The PSO algorithm represents the population as the term X, r_1 and r_2 represent random numbers, t represents the iteration number, C_1 and C_2 represent the coefficients of acceleration, and w is the inertia weight that is used to improve the speed of convergence. The inertia weight is calculated for each iteration using a linear deceasing inertia weight, which has the lowest inaccuracy compared to other inertia weights [22]:

$$X_i^{(g+1)} = X_i^{(g)} + V_i^{(g+1)} \quad (8)$$

where $X_i^{(g)}$ is the global best solution, and X_i^p is the best personal position. The above steps are performed until the stopping conditions are met.

$$w_i = w_{max} - \frac{w_{max} - w_{min}}{i_{max}} \times i \quad (9)$$

where w_{max} and w_{min} are the maximum and minimum inertia weights, respectively, and i represents the particle index.

2.6. Modeling of system components

The modeling of the mini-grid components is a significant step in the optimization for different configurations. The mathematical modeling of each mini-grid component is described in the next section.

2.6.1. Modeling the solar PV output

The power of a solar PV array as a function of the solar irradiance and the ambient temperature is defined by Eq. (10) [47].

$$P_{pv} = \theta_t \times PVA \times \mu_c(t) \quad (10)$$

where θ_t is the average irradiance in hour t, PVA is the surface size of the cell, and $\mu c(t)$ is the instantaneous PV cell efficiency.

However, solar PV generation cannot generate a constant electrical power output. Therefore, a probabilistic model of PV output, the Beta

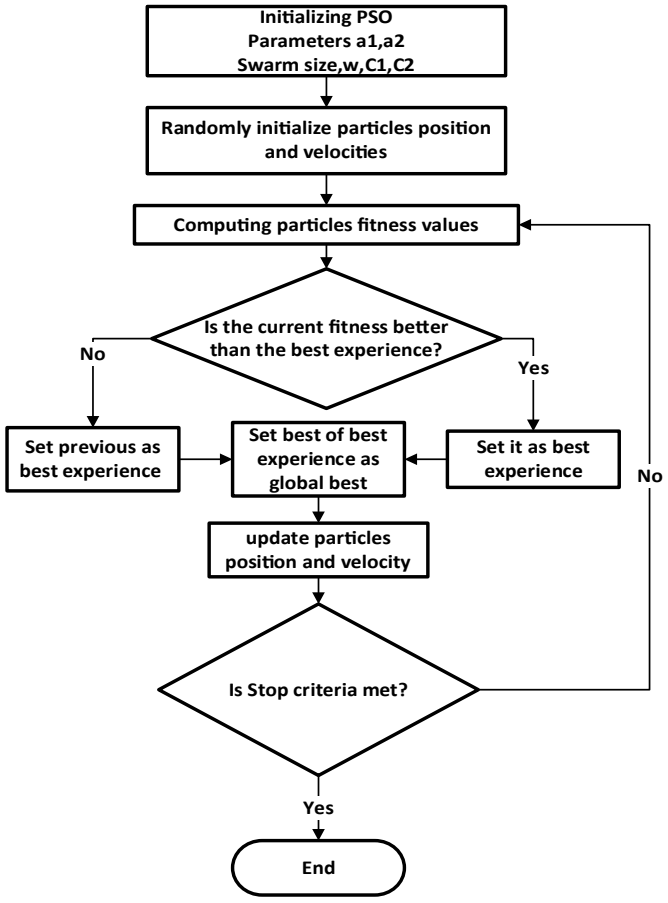

Fig. 4. Flowchart for the PSO algorithm.

PDF, is used to model the distribution of the solar irradiance, as shown in Eq. (11): [17].

$$f(\theta)\begin{cases}\dfrac{\Gamma(\alpha)\Gamma(\beta)}{\Gamma(\alpha)+\Gamma(\beta)}\theta^{\alpha-1}(1-\theta)^{\beta-1} & 0\le\theta\le 1,\alpha\ge 0,\beta\ge 0\\ 0 & otherwise\end{cases} \tag{11}$$

where α and β are elements of the Beta distribution function. The μ and σ terms represent the mean and standard deviation of the Beta PDF, respectively.

The probability of the solar irradiance θ can be calculated using Eq. (12):

$$P(\theta)=\int_{\theta_c}^{\theta_d} f(\theta)d\theta \tag{12}$$

The instantaneous PV cell efficiency can be calculated in terms of the cell temperature as [46]:

$$\mu_c(t)=\mu_{cr}[1-\beta_t(T_c(t)-T_{cr})] \tag{13}$$

where β_t is the temperature coefficient, in the range of 0.004–0.006 for silicon cells. The terms μ_{cr} and T_{cr} are the theoretical solar cell efficiency and temperature, respectively.

The value of *PVA*, which is the total solar cell area required to supply the load demand, can be calculated from Eq. (14):

$$PVA=\frac{1}{24}\sum_{t=1}^{24}\frac{P_{L,av}(t)F_s}{H_t\mu_c(t)\eta_{pc}V_F} \tag{14}$$

where F_s is the safety factor, which includes the possible allowance of insolation data inaccuracy, V_F is the factor of variability, which considers the impact of yearly radiation variation, and η_{pc} is the power conditioning system efficiency [45].

2.6.2. Battery energy storage (BES)

BES charging and discharging depends on the energy production and state of the charge of the BES at any given time. The state of the charge of the BES at a specified time is expressed by Eq. (15) and Eq. (16) [45]:

$$SOC(t+1)=SOC(t)(1-\sigma)+P_B(t)\eta_B \quad \text{charging mode} \tag{15}$$

$$SOC(t+1)=SOC(t)(1-\sigma)-P_B(t)/\eta_B \quad \text{discharging mode} \tag{16}$$

$$\text{where } P_B(t)=P_{PV}(t)-\frac{P_{HPL}(t)}{\eta_{inv}} \tag{17}$$

$P_{PV}(t)$ and $P_{HPL}(t)$ are the total power levels produced by the mini-grid system and required by the HPL at time *t*, respectively, *SOC* is the state of charge of the BES, η_B is the efficiency of the BES, and σ is the BES self-discharge rate. $P_B(t)$ represents the charging or discharging power of the BES at time *t*.

2.6.3. Power inverter

Inverters, which are responsible for converting DC to AC, is calculated using Eq. (18) [47]:

$$P_{inv}=\frac{P_{peak}}{\eta_{inv}} \tag{18}$$

where P_{peak} is the peak of the load demand, and η_{inv} is the efficiency of the inverter.

2.6.4. Diesel generator model

A DG is used to meet the HPLs in case the energy provided by the solar PV and BES is insufficient. The amount of fuel consumed by the DG depends upon its output power at each time-step [45]:

$$D_f(t)=\alpha_D P_{Dg}(t)+\beta_D P_{Dgr} \tag{19}$$

where $D_f(t)$ is the hourly fuel consumption of the DG, P_{Dg} is the average power per hour of the DG, P_{Dgr} is the rated power of the DG, and α_D and β_D are the coefficients of the fuel consumption curve.

2.6.5. Demand modeling

In the modeling of the electricity demand, uncertainties related to the demand are modeled using a normal distribution function [17]:

$$f_{load}(L_d)=\frac{1}{\sqrt{2\pi\sigma_{L_d}{}^2}}exp\left(-(L_d-L_{d_{mean}})^2/2\sigma^2 L_d\right) \tag{20}$$

3. Data used

The Bada village was selected as a case for this study. It is situated in a rural setting in the Afar region of northeastern Ethiopia (latitude, 14.309° and longitude, 40.072°). The village is currently non-electrified. It has been selected by the EEU for implementation of an autonomous, solar PV-based mini-grid. The weather data for the village collected from the Photovoltaic Geographical Information System (PVGIS) are shown in Fig. 5 [48]. Weekly load profiles, estimated based on interview data collected by EEU (as described in Section 2.1), are shown in Fig. 6.

Based on the data collected by the EEU and the load categorization described in Section 2.1, the load categorization for Bada village is shown in Table 1.

For the weekly load profile estimation, the following assumptions are applied: for water pumping, a minimum demand of 100 L of water per day per family and 2400 L/day for a health center and a primary school, each [12], and for the miller load profile estimation, two market days

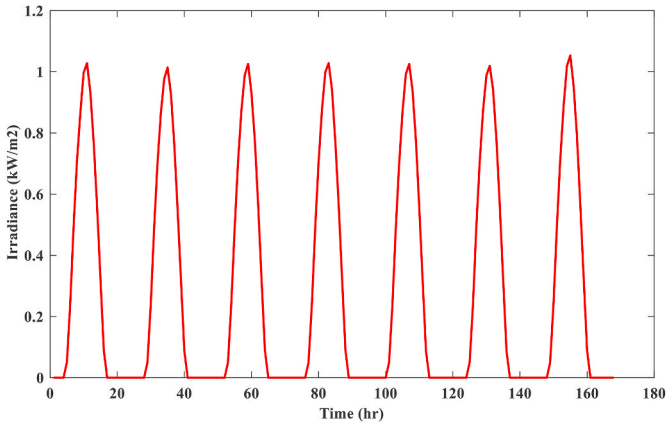

Fig. 5. Insolation profile of the Bada village.

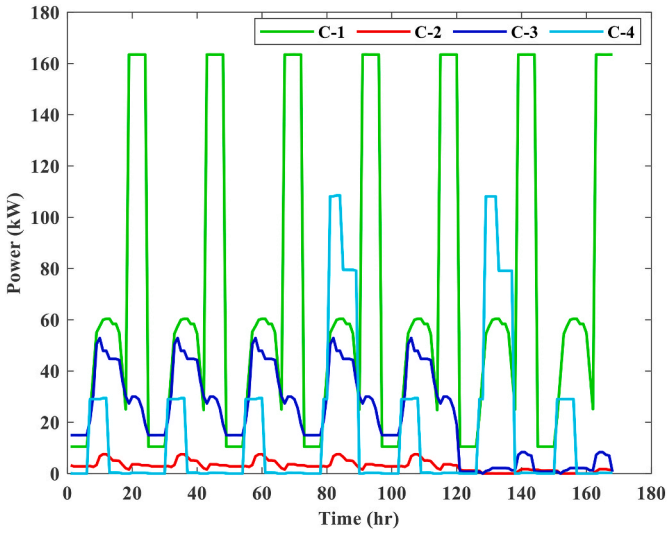

Fig. 6. Weekly load curves for the different load categories in the Bada village.

Table 1
Load categories for Bada village.

Load categories	Number and types of loads
C-1	2500 households
C-2	One clinic, One health center, One animal clinic, four pharmacies, two kindergartens, two elementary schools, four mosques, eight government offices, one farmer training center, and two storehouses
C-3	200 mini-shops, 1 barber, 10 tailors, 8 hotels, and 1 video hall
C-4	Five flour millers, and one water pump

(Thursday and Saturday).

3.1. Economic and technical parameters of the mini-grid components

The economic and technical parameters of the mini-grid components used are listed in Table 2. The fuel price considered is 0.62 $/L. Uncertainty levels of 5% and 11% are considered for the solar irradiance and load profile estimation, respectively. Other assumptions applied are an interest rate of 7% [49], inflation rate of 8.1%, and a project lifetime of 25 years [14].

When sizing the autonomous mini-grid components, the parameters used for the PSO algorithm are: particle size (n) of 100, maximum inertia weight of 0.9, and minimum inertia weight (w_{min}) of 0.4, since the inertia weight from 0.9 to 0.4 provides the best result as demonstrated by experimental testing [22]. To balance particle and global best, the acceleration factors c_1 and c_2 are set to the same value, 2. A maximum of 100 iterations (max_{ite}) is used as a stopping criterion.

4. Results and analysis

In this study, based on the sizing of the autonomous mini-grid components, the impacts of DSM implementation at category level on the cost-efficiency of an autonomous mini-grid in a non-electrified rural area are determined. The impacts of DSM implementation at the category level are also compared with load flexibility based on the sizing of the autonomous mini-grid components. To determine the optimal, cost-efficient sizes of the autonomous mini-grid components, calculated using Eq. (1), Eq. (10), Eq. (17) and Eq. (19), for each combination of the four load categories with DSM and different percentages of load flexibility, a PSO algorithm is used.

4.1. Impact of DSM implementation at category level on the cost-efficiency of mini-grids

The optimal sizes of the autonomous mini-grid components for each combination of load categories with implemented DSM in Configurations 1 and 2 are shown in Fig. 7a and b. The size of the BES, charged during higher levels of solar PV power production and discharged during peak demand hours, is highly influenced by the shiftable loads through the DSM implementation, as compared with the sizing of solar PV and DG.

As shown in Fig. 7a and b, different load categories with DSM have different impacts on the BES, solar PV, and DG sizing. In both configurations, DSM implementation in all load categories will result in reduced power from solar PV (391.6 kW) and no need for BES, since all loads are LPLs and are scheduled for hours with higher production of solar PV power. In Configuration 2, DSM implementation in all load categories results in no need for DG, thereby reducing the levels of CO_2 emissions and operational costs. The optimal sizes of the BES and solar PV in the No DSM case (base case), whereby all loads are HPLs and operate at their scheduled times, are 1584 kWh and 491.8 kW in Configuration 1 and 1491 kWh and 476.5 kW in Configuration 2, respectively.

Among the load categories, DSM implementation in C-1 has a greater impact than the other load categories, reducing the BES and solar PV by 1224 kWh (77.2%) and 81.5 kW (16.5%) in Configuration 1, and by

Table 2
Economic and technical parameters of the mini-grid components.

Component, unit	Price ($)	OMC ($/year)	RC ($)	T(year)	Nrep	SV[a] (%)	Reference
Solar PV, kW	1500	50	300	25	0	10	[50]
Civil Work, solar PV, kW	40%	1%	40%	25	0	20	[45]
Inverter, kW	711	0	650	10	2	10	[45]
BES, kWh	330	0	330	10	2	20	[51]
DG, kW	850	20	800	10	2	20	[38]

[a] SV is value of a scrap of the mini-grid components.

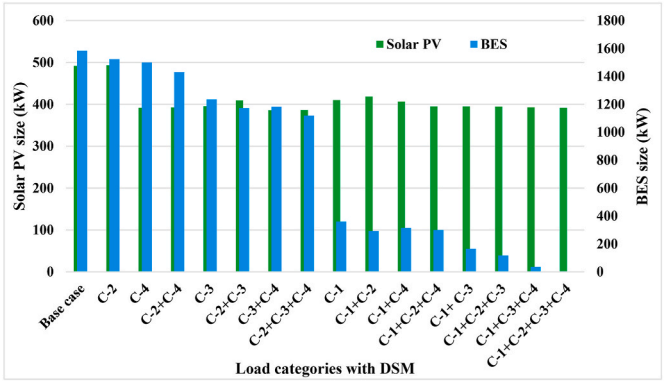

(a)

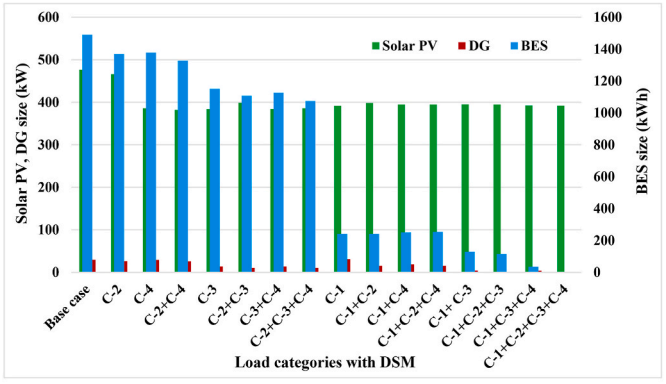

(b)

Fig. 7. Optimal component sizes for different load categories with DSM in: (a) Configuration 1; and (b) Configuration 2.

1249 kWh (83.7%) and 85 kW (17.8%) in Configuration 2, respectively, as compared to the No DSM case. DSM implementation in C-3, C-4, and C-2, in descending order of impact, reduces the optimal BES size by 21.9%, 5.3%, and 3.7%, respectively, as compared to the No DSM case, as shown in Fig. 7a. DSM implementation in C-3 and C-4 reduces the optimal solar PV size by 19.6% and 20.3%, respectively, as compared to the No DSM case. However, for DSM implementation in C-2, the optimal solar PV size is nearly equal to that in the No DSM case. In C-2, community load, demand is concentrated to the daytime, when there is a higher level of solar PV power production. This indicates that the shifting strategy has a lower impact for C-2.

In Configuration 2, DSM implementation reduces the optimal BES size by 22.7%, 7.5%, and 8%, and the optimal solar PV size by 19.4%, 19%, and 2.1% for C-3, C-4, and C-2, respectively, as compared to the No DSM case, as shown in Fig. 7b.

DSM implementation in C-3, with peak demand coinciding with solar PV power production, results in lower DG size than for other load categories, as shown in Fig. 7b. In the No DSM case, the optimal DG size is 29.5 kW, which is only 6% of the solar PV size, whereas DSM implementation in C-1, C-3, C-4, and C-2 results in optimal DG sizes of 31 kW, 14 kW, 29 kW, and 26 kW, respectively.

The LEC values, calculated using Eq. (2), for Configuration l (LEC-1) and Configuration 2 (LEC-2) are shown in Fig. 8. In Configuration 2, DG supplies peak loads. As a result, the BES and solar PV needed to meet peak loads are reduced, resulting in a lower LEC, thus LEC-2 is lower than LEC-1. DSM implementation in C-1, greatly reduces the size of the BES and reduces the levels of solar PV and DG more than in other load categories, leads to a dramatic decrease in LEC: LEC-1 is reduced by 45.8% and LEC-2 by 47.6%, as compared to the No DSM case. DSM implementation in C-3, C-4, and C-2 reduces the LEC-1 by 20.7%, 13%, and 1.6%, and LEC-2 by 21.8%, 13.2%, and 5.1%, respectively,

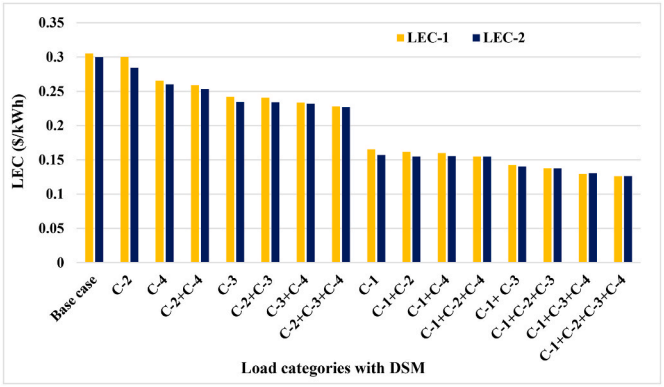

Fig. 8. LEC-1 and LEC-2 values for different load categories with DSM.

compared to the No DSM case.

4.2. Impact of load flexibility on the cost-efficiency of mini-grids

To determine the impact of load flexibility on the cost-efficiency of mini-grids, different levels of load flexibility, calculated using Eq. (1) and considering LPL in the implemented DSM operating strategy, are used in the optimal component sizing for Configurations 1 and 2, as shown in Fig. 9a and b. The BES size is particularly strongly influenced by load flexibility and is reduced, on average, by 29.8% for every 10% increase in load flexibility for both configurations, resulting in no need for BES for 100% load flexibility (an ideal case).

The optimal solar PV size is reduced, on average, by 2.1% for every

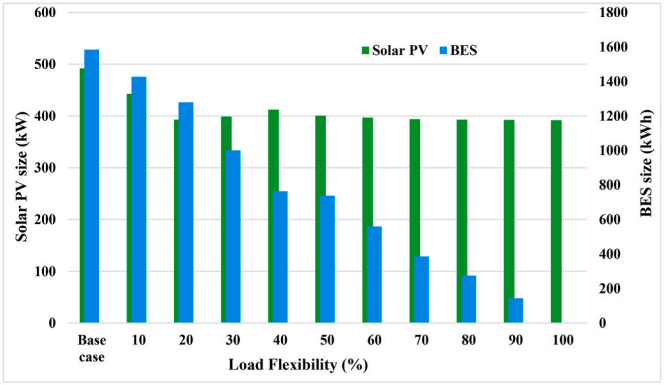

(a)

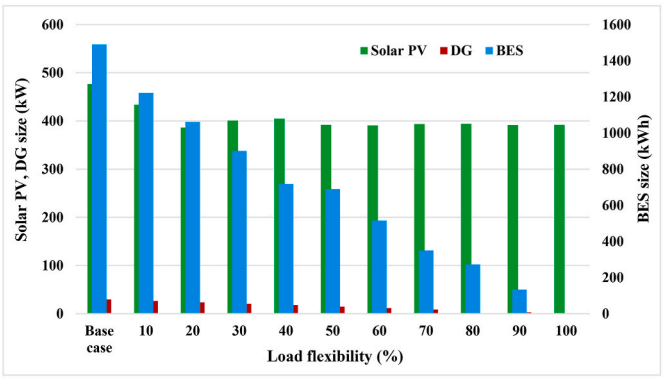

(b)

Fig. 9. Optimal component sizes for different percentages of load flexibility in: (a) Configuration 1; and (b) Configuration 2.

10% increase in load flexibility in Configuration 1, Fig. 9a, and in Configuration 2, Fig. 9b, on average by 1.8%. DG, which is only available in Configuration 2, is reduced, on average, by 12.1% for every 10% increase in load flexibility.

The impacts of load flexibility on the LEC values for Configuration 1 (LEC-1) and Configuration 2 (LEC-2) are shown in Fig. 10. Load flexibility reduces the LEC by, on average, 8.4% and 8.2% for every 10% increase in load flexibility for Configurations 1 and 2, respectively.

4.3. Comparison of the impacts of DSM implementation at category level and load flexibility on the cost-efficiency of mini-grids

As shown in Figs. 8 and 10, DSM implementation at category level has the same impact as that achieved by using a higher load flexibility. The DSM implemented in all the load categories reduces the LEC-1 by 58.7% and LEC-2 by 58%, as compared to the No DSM case, shown in Fig. 8. This is equal to the result for 100% load flexibility, Fig. 10.

The DSM implementation in C-1, Fig. 8, reduces LEC-1 and LEC-2 to almost the same extent as 55% and 58% load flexibility for Configurations 1 and 2 respectively, Fig. 10. C-3, C-4, and C-2, Fig. 8, have the capacity to reduce the LEC to almost the same extent as 25%, 16%, and 2% load flexibility for Configuration 1, and 26%, 16%, and 6% load flexibility for Configuration 1, respectively, Fig. 10.

In addition, as shown by comparison of Figs. 8 and 10, the difference between LEC-1 and LEC-2 diminishes with shiftable load categories, LPL, and percentage of load flexibility. This indicates that as shiftable load categories and load flexibility increases, DSM implementation will increase the cost-competitiveness of a 100% RES-based autonomous grid (Configuration 1).

4.4. Comparison of mini-grid sizing with and without considering uncertainty and validation of the PSO result

The optimal size of the mini-grid with and without consideration of load and supply side uncertainties for Configuration 1 and 2 is shown in Appendix B. Optimal sizing without considering uncertainties reduces the size of the BES and DG more than the solar PV, as shown in Appendix B since peak load variations caused by uncertainties is met by BES and DG. In Configuration 1, the optimal size of the BES and the solar PV are reduced by 3.2% and 2.4%, and in Configuration 2 by 2.5%, 2.6%, and 2.6% for the BES, solar PV, and DG, respectively.

The optimal size of the mini-grid for resulting from the use of an iterative method in the case of 10% load flexibility is shown in Appendix B. In finding the cost optimal size of the mini-grid components, the results obtained from the PSO algorithm and the iterative method are almost the same for both configurations, but the accuracy of the optimal solution differs. The convergence characteristics of the PSO algorithm for the optimal sizing with and without considering uncertainty is shown in Appendix C. As shown in the convergence characteristics of the PSO, the LCE decreases as the number of iterations increases and finally converges to the optimal value.

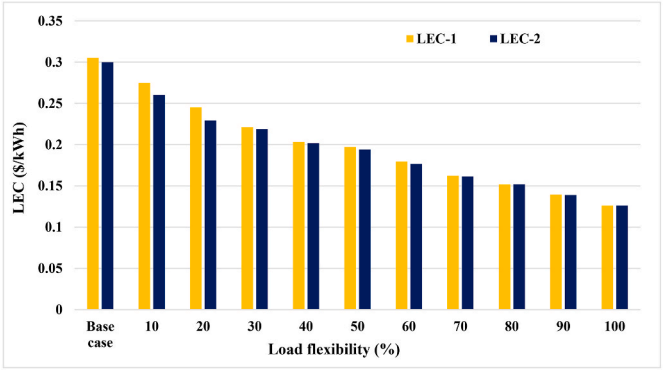

Fig. 10. LEC-1 and LEC-2 values for different percentages of load flexibility.

5. Discussion

The impacts of DSM implementation using a load-shifting strategy on the cost-efficiency of autonomous mini-grids in non-electrified rural areas were determined. The impact was determined at category level rather than at appliance level for four load categories with different load profiles. This is a novelty, since previous similar studies have determined the impact at appliance level.

The component sizing was carried out for each combination of the four load categories using a PSO algorithm. Load-side and supply-side uncertainties were also considered, but not their development with time. The applied load-shifting strategy was conducted in a priority-based fashion, with Configuration 1 supplying HPLs at the scheduled time and LPLs only when there is sufficient power generation from solar PV and the BES is full. In Configuration 2, the HPLs were supplied using the DG when neither solar PV generation nor BES is sufficient.

In contrast to the day-ahead DSM strategy, which has been studied to determine the optimal time when LPLs can be curtailed for higher levels of user satisfaction [27], the load-shifting strategy applied in this study does not include load curtailment, thus increasing system reliability. However, the results of the study are in line with those of previous studies [11,28–30], regarding how the cost-efficiency of mini-grids is impacted by a priority-based shifting strategy.

The results show that different category combinations result in large variability in terms of possible LEC reductions and, thus, in terms of the optimal sizing of cost-efficient BES, solar PV, and DG. This indicates that the cost-effectiveness of rural mini-grid depends on the load category mix considered for HPL and LPL when DSM is implemented.

Considering the order of impact among the load categories in terms of creating a cost-efficient mini-grid, C-1, the household category, is the most significant followed by C-3, the productive use category, followed by C-2 and C-4. Due to their load profiles, the capacity of the DSM implementation in C-1 and C-3 to reduce the LEC is almost equal to the impacts achieved by 55% and 25%, and 58% and 26% load flexibility for solar PV-based and HRES-based autonomous mini-grids, respectively. C-1 and C-3 are the main contributors to the night-time peak demand when there is no solar PV power production and, thus, more BES is required to ensure the supply. C-2 and C-4, on the other hand, have peak demand during the daytime, when there is higher solar PV power production. However, C-2 + C-4 have a higher peak and energy demand than C-2 and C-4, resulting in a lower LEC than C-2 and C-4, but higher than C-1 and C-3. Thus, the implementation of a load-shifting strategy in these categories would have a weaker impact on reducing the BES size and, therefore, a weaker impact on the LEC.

In Configuration 1 and 2, the productive use category, C-3, with a night time load, have a greater impact on the cost-efficiency of mini-grids than productive use category, C-4, without night time load. This indicates that productive loads can increase the cost-efficiency of mini-grids [52,53], but not all productive loads have equal impact. The impact of DSM implementation in C-1, reducing the size of the autonomous mini-grid components and the LEC, will likely become more important with each year due to the pronounced increase in household connections compared to other types of loads in rural areas [27]. While C-3 has a weaker impact than C-1, it has the capacity to increase the load factor of the mini-grid and improve the cost-efficiency of the mini-grid [52]. However, balancing different load categories is an important factor, in addition to DSM implementation at the category level to create a cost-efficient mini-grid in rural areas [53].

The variation in LEC reduction observed for the different categories indicates that different tariff structures, based on category level, would be required for system operation. Thus, DSM implementation at category level can be used with smart pricing methods such as time of use (TOU) electricity tariffs, which are more effective in mini-grids that have

poor availability of skilled personnel [26] and have the capacity to handle voltage dip and power deviations in mini-grids [17]. DSM with a TOU electricity tariff enables the control of each load category based on its load profiles, using different electricity tariffs for different load categories at different times of the day. However, system operators can choose a type of DSM implementation that reflects their own perspectives. Importantly, depending on the ownership and business model of the mini-grid, the relationship between the utility and its customers may differ significantly, including in relation to the priority given to the load categories [54].

DSM implementation requires use of communication infrastructure and distributed smart meters that sense and control the electricity usage. As the users number increases, and thus system complexity, this need increases exponentially [55]. However, less infrastructure is needed at category level than at appliance level. This indicates that DSM at category level in rural mini-grids will reduce the operational and maintenance challenges by decreasing the complexity linked to controlling and connecting appliances, which is associated with appliance level DSM implementation [11,28–30].

In category level DSM implementation, aggregated load estimations are sufficient [56].Thus, DSM implementation at category level is less impacted by load estimation uncertainties since over and under appliance load estimations offset each other [57].

DSM implementation in C-1, followed by C-3, C-4, and C-2 in order of impact, increases the cost-competitiveness of solar PV-based, 100% RES, autonomous mini-grids by significantly reducing the BES and reducing the solar PV size. In this way, DSM contributes to decarbonization of the energy sector by promoting 100% RES-based autonomous mini-grids.

The contribution of DSM to energy sector decarbonization indicates a need for policies encouraging implementation of DSM in C-1 and C-3 rather than in C-4 and C-2 for rural area electrification using 100% RES-based autonomous mini-grids. This also indicates that DSM applied in combination with RETs subsidies creates options for 100% RES-based rural area electrification.

DSM implementation at category level requires a reduction in the level of consumption by users, which certainly is a limitation to its application. In C-1, lighting is one of the main reasons for the night-time peak demand, and reduced lighting is required to create a cost-efficient autonomous mini-grid. In addition to C-1, C-3 also requires decreased consumption from LPLs such as TVs, refrigerators, radios, mobile charging, and other appliances used for entertainment. As a result, the creation of more-cost-efficient autonomous mini-grids by DSM implementation at category level will require decreased user consumption, in turn, affecting user satisfaction.

Further studies of DSM implementation at category level could involve increased categorization and load prioritization, as well as implementation of other DSM strategies, e.g., the use of different tariff settings in demand response programs, consideration of user satisfaction and integration of alternative storage systems, such as pumped hydro storage.

6. Conclusions

In this study, we investigate ways in which DSM implementation contributes to cost-efficient, autonomous mini-grids in non-electrified rural areas. DSM exerts impacts on four load categories through a load-shifting strategy. The results show that DSM implementation has a stronger impact on reducing BES than solar PV and the use of a diesel-fueled generator. Load categories C-1 (household) and C-3 (productive use) show the highest cost-efficiency impacts, reducing the LEC to extents that are almost equal to those achieved by 55% and 25%, and 58% and 26% load flexibility for solar PV-based and HRES-based autonomous mini-grids, respectively. In comparison to DSM implementation in C-1 and C-3, implementation in C-4 and C-2 have lower impacts. However, C-4 and C-2 can reduce LEC to almost the same extent as achieved by 16% and 2% load flexibility for solar PV-based autonomous mini-grids, and 16% and 6% load flexibility for HRES-based autonomous mini-grids, respectively. Therefore, DSM implementation in C-1 and C-3 will increase the cost-competitiveness of 100% RES-based autonomous mini-grids in non-electrified rural areas, as compared to the C-4 and C-2 load categories. The study adds methodological novelty through its approach of investigating mini-grid DSM implementation impacts at the category level.

Declaration of competing interest

The authors declare that they have no known competing financial interests or personal relationships that could have appeared to influence the work reported in this paper.

Data availability

Data will be made available on request.

Acknowledgments

We thank the Swedish International Development Cooperation Agency (SIDA) for providing financial support for this research, and the Ethiopian Electric Utility (EEU) for valuable information and data.

Appendix A. Used equations

$$CRF = \frac{r(1+r)^T}{(1+r)^T - 1}$$

$$IOMC = OMC_0\left(\frac{1+i}{r-i}\right)\left(1-\left(\frac{1+i}{1+r}\right)^T\right) \quad r \neq i$$

$$OMC = OMC_0 \times T \quad r = i$$

$$RC = \sum_{j=1}^{N_{rep}}\left(C_{RC} \times C_V \times \left(\frac{1+i}{1+r}\right)^{\frac{Tsj}{(N_{rep}+1)}}\right)$$

$$PSV = \sum_{j=1}^{N_{rep}+1} SV\left(\frac{1+i}{1+r}\right)^{\frac{Tsj}{N_{rep}+1}}$$

$$SOC(t+1) = SOC(t)(1-\sigma)$$

$$SOC_{min} = (1 - DOD)C_B$$

$$\beta = (1-\mu) \times \left(\frac{u \times (1+\mu)}{\sigma^2} - 1\right)$$

$$\alpha = \frac{\mu \times \beta}{1-u}$$

$$T_c(t) = T_a + 3H_t(t)$$

Appendix B. Optimal size of mini grid with and without considering uncertainty using PSO and Iterative method

Component, unit	Configuration 1			Configuration 2		
	With uncertainty		Without uncertainty	With uncertainty		Without uncertainty
	Iteration	PSO	PSO	Iteration	PSO	PSO
Solar PV, kW	441.6	442.6	432.1	441.6	433.5	422.9
BES, kWh	1446	1425	1380	1410	1221.5	1189.9
DG, kW	0	0	0	26.5	26.5	25.8

Appendix C. Convergence characteristics of the PSO algorithm

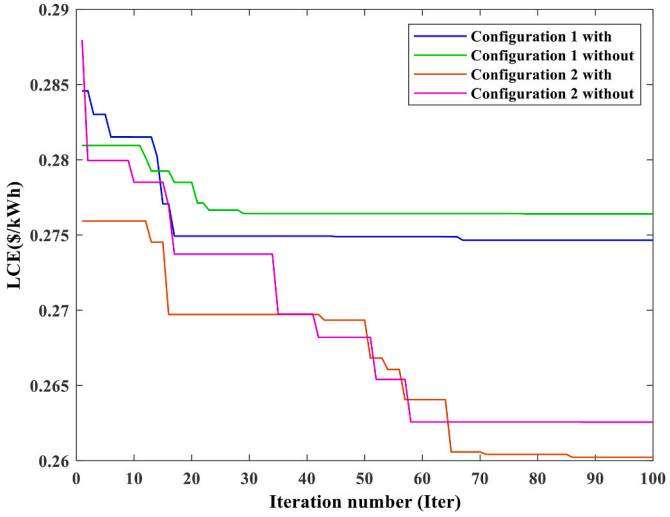

References

[1] Transforming UN. Our world: the 2030 agenda for sustainable development. In: Sustainable development knowledge Platform; 2015. p. 41. United Nations, https://sustainabledevelopment-un-org.acces.bibl.ulaval.ca/post2015/transformingourworld/publication. [Accessed 7 June 2022].

[2] Wright VP. World energy outlook. 1986. 23–8.

[3] Abada I, Othmani M, Tatry L. An innovative approach for the optimal sizing of mini-grids in rural areas integrating the demand, the supply, and the grid. Renew Sustain Energy Rev 2021;146:111117. https://doi.org/10.1016/J.RSER.2021.111117.

[4] Mini ESMAP. Grids for half a billion people: market outlook and handbook for decision makers. 2019.

[5] Nguyen TA, Crow ML, Elmore AC. Optimal sizing of a vanadium redox battery system for microgrid systems. IEEE Trans Sustain Energy 2015;6:729–37. https://doi.org/10.1109/TSTE.2015.2404780.

[6] Tuballa ML, Abundo ML. A review of the development of Smart Grid technologies. Renew Sustain Energy Rev 2016;59:710–25. https://doi.org/10.1016/J.RSER.2016.01.011.

[7] Dileep G. A survey on smart grid technologies and applications. Renew Energy 2020;146:2589–625. https://doi.org/10.1016/J.RENENE.2019.08.092.

[8] Baurzhan S, Jenkins GP. Off-grid solar PV: is it an affordable or appropriate solution for rural electrification in Sub-Saharan African countries? Renew Sustain Energy Rev 2016;60:1405–18. https://doi.org/10.1016/J.RSER.2016.03.016.

[9] Girma M, Assefa A, Molinas M, Girma M, Assefa A, Molinas M. Feasibility study of a solar photovoltaic water pumping system for rural Ethiopia. AIMS Environ Sci 2015;2:697–717. https://doi.org/10.3934/ENVIRONSCI.2015.3.697.

[10] Aziz S, Chowdhury SA. Performance evaluation of solar mini-grids in Bangladesh: a two-stage Data Envelopment Analysis. Clean Environ Syst 2021;2:100003. https://doi.org/10.1016/J.CESYS.2020.100003.

[11] Akram F, Asghar F, Majeed MA, Amjad W, Manzoor MO, Munir A. Techno-economic optimization analysis of stand-alone renewable energy system for remote areas. Sustain Energy Technol Assessments 2020;38:100673. https://doi.org/10.1016/J.SETA.2020.100673.

[12] Nkiriki J, Ustun TS. Mini-grid policy directions for decentralized smart energy models in Sub-Saharan Africa. IEEE PES Innov Smart Grid Technol Conf Eur 2017:1–6. https://doi.org/10.1109/ISGTEUROPE.2017.8260217.

[13] Amara S, Toumi S, Salah C Ben. A comparison of optimal sizing methods for Microgrid applications and description of a proposed iterative algorithm. IEEE 21st Int Ccnference Sci Tech Autom Control Comput Eng 2022. https://doi.org/10.1109/STA56120.2022.10019238. 2022:654–9.

[14] Kebede KY. Viability study of grid-connected solar PV system in Ethiopia. Sustain Energy Technol Assessments 2015;10:63–70. https://doi.org/10.1016/j.seta.2015.02.003.

[15] Suryoatmojo H, Elbaset A. Syafaruddin and T. Hiyama "genetic algorithm based optim sizing PV–Wind–Diesel–Hydrogen–Battery. Syst Innov Comput Inf Control 2010;6.
[16] Kamjoo A, Maheri A, Dizqah AM, Putrus GA. Multi-objective design under uncertainties of hybrid renewable energy system using NSGA-II and chance constrained programming. Int J Electr Power Energy Syst 2016;74:187–94. https://doi.org/10.1016/j.ijepes.2015.07.007.
[17] Huang S, Abedinia O. Investigation in economic analysis of microgrids based on renewable energy uncertainty and demand response in the electricity market. Energy 2021;225:120247. https://doi.org/10.1016/J.ENERGY.2021.120247.
[18] Anand P, Rizwan M, Bath SK. Sizing of renewable energy based hybrid system for rural electrification using grey wolf optimisation. Approach 2019;1:158–72. https://doi.org/10.1049/iet-esi.2018.0053.
[19] Nolan S, Strachan S, Rakhra P, Frame D. Optimized network planning of mini-grids for the rural electrification of developing countries. Proc - 2017 IEEE PES-IAS PowerAfrica Conf Harnessing Energy, Inf Commun Technol Afford Electrif Africa 2017:489–94. https://doi.org/10.1109/PowerAfrica.2017.7991274.
[20] Kumar S, Kaur T, Upadhyay S, Sharma V, Vatsal D. Optimal sizing of stand alone hybrid renewable energy system with load shifting. ENERGY SOURCES, PART A Recover Util Environ Eff 2020:1–20. https://doi.org/10.1080/15567036.2020.1831107.
[21] Mohamed MA, Eltamaly AM, Alolah AI. Swarm intelligence-based optimization of grid-dependent hybrid renewable energy systems. Renew Sustain Energy Rev 2017;77:515–24. https://doi.org/10.1016/J.RSER.2017.04.048.
[22] Bansal JC, Singh PK, Saraswat M, Verma A, Jadon SS, Abraham A. Inertia weight strategies in particle swarm optimization. Proc 2011 3rd World Congr Nat Biol Inspired Comput NaBIC 2011. https://doi.org/10.1109/NaBIC.2011.6089659.
[23] Khezri R, Razmi P, Mahmoudi A, Bidram A, Khooban MH. Machine learning-based sizing of a renewable-battery system for grid-connected homes with fast-charging electric vehicle. IEEE Trans Sustain Energy 2022;14:1949–3029. https://doi.org/10.1109/TSTE.2022.3227003.
[24] Ela E, Diakov V, Ibanez E, Heaney M. Impacts of variability and uncertainty in solar photovoltaic generation at Multiple timescales. 2013. p. 1–41. https://doi.org/10.2172/1081387.
[25] Mehrjerdi H, Hemmati R. Energy and uncertainty management through domestic demand response in the residential building. Energy 2020;192:116647. https://doi.org/10.1016/J.ENERGY.2019.116647.
[26] Shakya B, Bruce A, MacGill I. Survey based characterisation of energy services for improved design and operation of standalone microgrids. Renew Sustain Energy Rev 2019;101:493–503. https://doi.org/10.1016/J.RSER.2018.11.016.
[27] Rajbhandari Y, Marahatta A, Shrestha A, Gachhadar A, Thapa A, Gonzalez-Longatt F, et al. Load prioritization technique to guarantee the continuous electric supply for essential loads in rural microgrids. Int J Electr Power Energy Syst 2022;134:107398. https://doi.org/10.1016/j.ijepes.2021.107398.
[28] Derakhshan G, Shayanfar HA, Kazemi A. The optimization of demand response programs in smart grids. Energy Pol 2016;94:295–306. https://doi.org/10.1016/j.enpol.2016.04.009.
[29] Setlhaolo D, Xia X. Optimal scheduling of household appliances incorporating appliance coordination. Energy Proc 2014;61:198–202. https://doi.org/10.1016/j.egypro.2014.11.1062.
[30] Eltamaly AM, Mohamed MA, Al-Saud MS, Alolah AI. 1813–28. In: Load management as a smart grid concept for sizing and designing of hybrid renewable energy systems. 49; 2016. https://doi.org/10.1080/0305215X.2016.1261246.
[31] Wang X, Song W, Wu H, Liang H, Saboor A. Microgrid operation relying on economic problems considering renewable sources, storage system, and demand-side management using developed gray wolf optimization algorithm. Energy 2022;248:123472. https://doi.org/10.1016/J.ENERGY.2022.123472.
[32] Alahmed AS, Al-Muhaini MM. An intelligent load priority list–based integrated energy management system in microgrids. Elec Power Syst Res 2020;185:106404. https://doi.org/10.1016/J.EPSR.2020.106404.
[33] Zare Oskouei M, Sadeghi Yazdankhah A. The role of coordinated load shifting and frequency-based pricing strategies in maximizing hybrid system profit. Energy 2017;135:370–81. https://doi.org/10.1016/J.ENERGY.2017.06.150.
[34] Thakur J, Chakraborty B. Demand side management in developing nations: a mitigating tool for energy imbalance and peak load management. Energy 2016;114:895–912. https://doi.org/10.1016/J.ENERGY.2016.08.030.
[35] Yuan G, Gao Y, Ye B, Huang R. Real-time pricing for smart grid with multi-energy microgrids and uncertain loads: a bilevel programming method. Int J Electr Power Energy Syst 2020;123:106206. https://doi.org/10.1016/J.IJEPES.2020.106206.
[36] Dranka GG, Ferreira P, Vaz AIF. Integrating supply and demand-side management in renewable-based energy systems. Energy 2021;232:120978. https://doi.org/10.1016/J.ENERGY.2021.120978.
[37] Zizzo G, Beccali M, Bonomolo M, Di Pietra B, Ippolito MG, La Cascia D, et al. A feasibility study of some DSM enabling solutions in small islands: the case of Lampedusa. Energy 2017;140:1030–46. https://doi.org/10.1016/J.ENERGY.2017.09.069.
[38] Prathapaneni DR, Detroja KP. An integrated framework for optimal planning and operation schedule of microgrid under uncertainty. Sustain Energy, Grids Networks 2019;19:100232. https://doi.org/10.1016/J.SEGAN.2019.100232.
[39] Rajamand S. Effect of demand response program of loads in cost optimization of microgrid considering uncertain parameters in PV/WT, market price and load demand. Energy 2020;194:116917. https://doi.org/10.1016/J.ENERGY.2020.116917.
[40] Ahlborg H, Hammar L. Drivers and barriers to rural electrification in Tanzania and Mozambique – grid-extension, off-grid, and renewable energy technologies. Renew Energy 2014;61:117–24. https://doi.org/10.1016/J.RENENE.2012.09.057.
[41] Bhandari R, Sessa V, Adamou R. Rural electrification in Africa – a willingness to pay assessment in Niger. Renew Energy 2020;161:20–9. https://doi.org/10.1016/j.renene.2020.06.151.
[42] Askarzadeh A, dos Santos Coelho L. A novel framework for optimization of a grid independent hybrid renewable energy system: a case study of Iran. Sol Energy 2015;112:383–96. https://doi.org/10.1016/J.SOLENER.2014.12.013.
[43] Hartvigsson E, Ehnberg J, Ahlgren EO, Molander S. Linking household and productive use of electricity with mini-grid dimensioning and operation. Energy Sustain Dev 2021;60:82–9. https://doi.org/10.1016/j.esd.2020.12.004.
[44] Lorenzoni L, Cherubini P, Fioriti D, Poli D, Micangeli A, Giglioli R. Classification and modeling of load profiles of isolated mini-grids in developing countries: a data-driven approach. Energy Sustain Dev 2020;59:208–25. https://doi.org/10.1016/j.esd.2020.10.001.
[45] Abdelaziz Mohamed M, Eltamaly AM. A PSO-based smart grid application for optimum sizing of hybrid renewable energy systems. Stud Syst Decis Control 2018;121:53–60. https://doi.org/10.1007/978-3-319-64795-1_5.
[46] Elsheikh AH, Abd Elaziz M. Review on applications of particle swarm optimization in solar energy systems. Int J Environ Sci Technol 2019;16:1159–70. https://doi.org/10.1007/s13762-018-1970-x.
[47] Mohamed MA, Eltamaly AM, Alolah AI. Sizing and techno-economic analysis of stand-alone hybrid photovoltaic/wind/diesel/battery power generation systems. J Renew Sustain Energy 2015;7:063128. https://doi.org/10.1063/1.4938154.
[48] JRC photovoltaic geographical information system (PVGIS) - European commission n.d. https://re.jrc.ec.europa.eu/pvg_tools/en/#api_5.2. [Accessed 1 December 2022].
[49] National bank of Ethiopia 2017:1–3. https://market.nbebank.com/pdf/directives/bankingbusiness/Interest rate directive.pdf. [Accessed 7 June 2022].
[50] Khezri R, Mahmoudi A, Whaley D. Optimal sizing and comparative analysis of rooftop PV and battery for grid-connected households with all-electric and gas-electricity utility. Energy 2022;251:123876. https://doi.org/10.1016/J.ENERGY.2022.123876.
[51] Kiptoo MK, Lotfy ME, Adewuyi OB, Conteh A, Howlader AM, Senjyu T. Integrated approach for optimal techno-economic planning for high renewable energy-based isolated microgrid considering cost of energy storage and demand response strategies. Energy Convers Manag 2020;215:112917. https://doi.org/10.1016/J.ENCONMAN.2020.112917.
[52] van Hove E, Johnson NG, Blechinger P. Evaluating the impact of productive uses of electricity on mini-grid bankability. Energy Sustain Dev 2022;71:238–50. https://doi.org/10.1016/J.ESD.2022.10.001.
[53] Gelchu MA, Ehnberg J, Ahlgren EO, Hartvigsson E. Improving load factors as a smart management approach - a developing country mini-grid case study. PowerAfrica: IEEE PES/IAS PowerAfrica; 2021. https://doi.org/10.1109/POWERAFRICA52236.2021.9543147. 2021.
[54] Ehnberg J, Ahlborg H, Hartvigsson E. Flexible distribution design in microgrids for dynamic power demand in low-income communities. IEEE PES PowerAfrica Conf PowerAfrica 2016:179–83. https://doi.org/10.1109/POWERAFRICA.2016.7556596.
[55] Saeidpour Parizy E, Jahanbani Ardakani A, Mohammadi A, Loparo KA. A new quantitative load profile measure for demand response performance evaluation. Int J Electr Power Energy Syst 2020;121:106073. https://doi.org/10.1016/J.IJEPES.2020.106073.
[56] Hartvigsson E, Ahlgren EO. Comparison of load profiles in a mini-grid: assessment of performance metrics using measured and interview-based data. Energy Sustain Dev 2018;43:186–95. https://doi.org/10.1016/j.esd.2018.01.009.
[57] Blodgett C, Dauenhauer P, Louie H, Kickham L. Accuracy of energy-use surveys in predicting rural mini-grid user consumption. Energy Sustain Dev 2017;41:88–105. https://doi.org/10.1016/J.ESD.2017.08.002.